Approximating Complex Surfaces by Triangulation of Contour Lines

Abstract: An algorithm is described for obtaining an optimal approximation, using triangulation, of a three-dimensional surface defined by randomly distributed points along contour lines. The combinatorial problem of finding the best arrangement of triangles is treated by assuming an adequate objective function. The optimal triangulation is found using classical methods of graph theory. An illustrative example gives the procedure for triangulation of contour lines of a human head for use in radiation therapy planning.

Introduction

In many branches of applied science, an important problem concerns the mathematical description provided by a set of points on a three-dimensional surface. The choice between accurate but time-consuming surfacefitting procedures and the simpler but more flexible numerical approximation methods depends essentially on the practical needs and requirements in the field of application.

A specific area of biomedicine requiring surface approximation is computer-assisted three-dimensional radiation therapy planning [1]. Briefly, the aim of surface approximation in radiation treatment is as follows. The radiation energy absorbed by the body strongly depends on the thickness and the density of the tissue penetrated by the beam ray. The therapeutic irradiation of cancerous cells requires careful individual planning to ensure that despite the variations of the human anatomy the adequate dose of radiation covers the tumor volume to be treated, whereas the surrounding healthy tissue is properly spared excessive exposure. The planning necessitates the availability of a reliable individual geometrical model of the patient's body for a computer simulation of the treatment dosimetry.

In the routine practice of radiation therapy the accuracy of dosage calculations depends in large measure on the adequacy of the description of body irregularities

and of relevant heterogeneous zones, such as the lungs, bones or air gaps. The usual form under which anatomical measurements of a patient can be rapidly made available consists of body contour lines in several parallel planar cross sections drawn in life size on paper. The boundaries of important heterogeneities inside the body can be added from anatomical atlases and fitted to the proper scale with the help of x-ray photographs. For the digital handling of these curves a sequence of coordinates is carefully selected along the contour lines.

The major problem consists in the numerical representation of the anatomical boundaries in the computer. A compromise must be established between accuracy of approximation and simplicity of mathematical handling. A suitable approach for constructing a numerical model from the contour line measurements consists in the approximation of the anatomical boundaries by triangulation. This method, as shown in Fig. 1, consists in joining points of neighboring contour lines to triangles in such a manner that one obtains triangular planar elements which delimit a polyhedron approximating the surface of interest.

Although the advantages of this model for medical computing purposes were recognized some time ago [2], attempts at realization for three-dimensional therapy planning computations were abandoned because no reli-

able algorithm existed for triangulating complex surfaces satisfactorily in all cases.

The triangulation problem resides in the fact that contour lines do not contain sufficient information regarding the system of gradients associated with the surface they describe. Moreover, the combinatorial aspect of the problem becomes apparent when one considers how many different triangle arrangements T can be constructed for a fixed number of contour points. It can be shown that between two contour lines consisting of n and m points,

$$T(m, n) = [(m-1) + (n+1)]!/[(m-1)!(n-1)!].$$
(1)

The expression (1) demonstrates that for relatively few contour points, the number of possible triangle permutations is very large: According to (1), n = m = 12 points, for example, provides about 10^7 triangle combinations and thus different surface shapes. This example obviously precludes an exhaustive search for the optimal triangulation.

This paper describes a computer algorithm for finding an optimal approximation, using triangles, of a surface defined by a set of contour lines. Instead of giving a formal mathematical treatment of the problem, we present a simple and reliable computer method for triangulating arbitrary surfaces defined by randomly distributed points along the contours. This method is applicable without restriction to any contour lines twisted into convex and concave portions.

This new approach is described in the sections following. It consists in assuming an adequately simple objective function for the handling of the optimization problem. This combinatorial scheme of triangulation then permits resolution of the problem with known graphtheoretical techniques. In the last section an example of triangulating an anatomical surface illustrates the method.

Iteration scheme of the algorithm

We consider an unknown three-dimensional surface of interest for which a map of contour lines is given in a Cartesian coordinate system as shown in Fig. 1. A contour line represents a cross section of constant z value and is numerically provided by the x-y coordinates of an ordered, randomly distributed sequence of points on the contour line. The total number of contour points given depends in practice on the desired accuracy. The spacing between cross sections is assumed to be variable.

The main strategy for finding the optimal arrangement of triangles approximating the unknown surface is to decompose the given set of contour points into subsets such that a proper objective function may be stated separately for each subset.

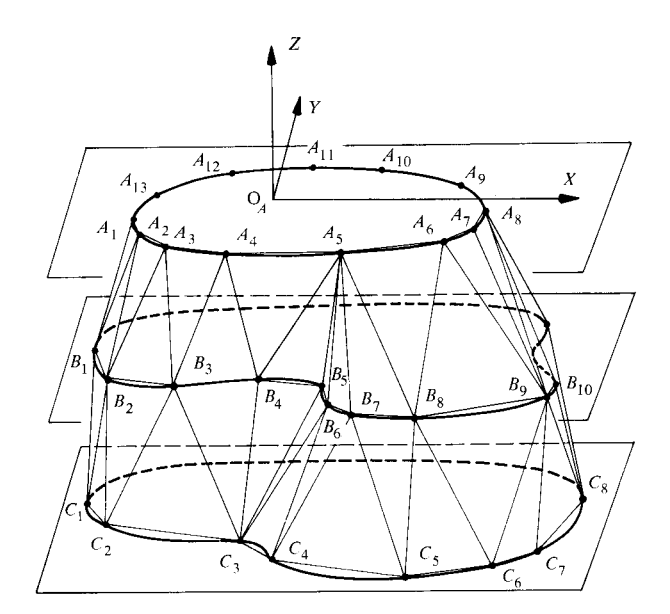


Figure 1 Method of approximating, by means of triangles, the surface of a volume defined by contour lines.

The first decomposition step consists in handling each pair of adjacent contour lines independently. When an object is defined by more than two cross sections, each lateral surface band delimited by two neighboring contour lines is triangulated separately, and the entire surface is obtained by handling subsequently all pairs of adjacent contour lines.

The decisive decomposition process finds application when arbitrarily flexed contour lines, i.e., with alternating sign of curvature, are handled. For simplicity of presentation, we first assume the contour lines to be closed and the contour points ordered in a positive, e.g., an anticlockwise, sequence. The sign of curvature is then conventionally fixed; a sequence of three consecutive contour points is convex if the curvature of the circle going through the three points has a positive sign and is concave otherwise. The triangulation of a pair of arbitrary contour lines is achieved by an iterative decomposition of the contour points into point subsets of exclusively convex or concave sequences, alternately. The example in Fig. 2 illustrates such a stepwise decomposition of a closed set S of contour points into purely convex and concave subsets S_i , $i = 1, 2, 3, \cdots$. The convex subset S_1 for the first iteration step is obtained by removing from S any point A_k for which the circle going through A_{k-1} , A_k and A_{k+1} has negative sign of curvature. Remaining point sequences are then tested for opposite sign of curvature in the same way, and the process is repeated until the contour points are separated into convex or concave sequences.

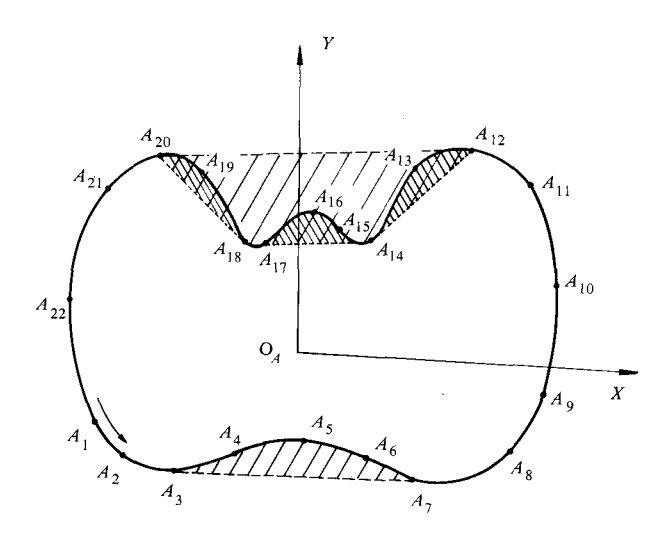


Figure 2 Example of iterative decomposition of a set of contour points $S = \{A_1, A_2, \cdots A_{22}\}$ into alternately concave and convex subsets.

- 1. convex subset $S_1 = \{A_1, A_2, A_3, A_7, A_8, A_9, A_{10}, A_{11}, A_{12}, A_{20}, A_{21}, A_{22}\}.$
- $\begin{array}{c} \text{2. concave subsets } S_{2}^{\ 1} = \{A_{3},\,A_{4},\,A_{5},\,A_{6},\,A_{7}\},\\ S_{2_{1}}^{\ 2} = \{A_{12},\,A_{14},\,A_{17},\,A_{18},\,A_{20}\}. \end{array}$
- 3. convex subsets $S_{3_2} = \{A_{12}, A_{13}, A_{14}\},$ $S_{3_2} = \{A_{14}, A_{15}, A_{16}, A_{17}\},$ and $S_{3_3} = \{A_{18}, A_{19}, A_{20}\}.$

A triangulation criterion for purely convex contour lines is now formulated. Let two convex sets of contour points $S^a = \{A_1, A_2, A_3, \dots, A_m\}$ and $S^b = \{B_1, B_2, B_3, \dots, B_n\}$, and a trial triangulation between them be given, as shown in Fig. 3. Let us consider the polyhedron $A_1A_2A_3$, \dots , $A_mB_1B_2B_3$, \dots , B_n originated by this triangle arrangement. We assume the following objective function for optimal triangulation of the two convex contour lines S^a and S^b .

The triangulation which maximizes the volume of the polyhedron $A_1A_2A_3, \dots, A_mB_1B_2B_3, \dots, B_n$ gives the optimal approximation of the surface provided by a pair of closed convex contour lines.

This objective function also extends obviously to concave contour point subsets. We consider Fig. 2 as an example of an arbitrarily flexed contour line, containing concave sequences of contour points. We suppose the volume of any polyhedron $A_1A_2A_3, \dots, A_mB_1B_2B_3, \dots, B_n$ to be algebraically oriented such that the volume is positive for an anticlockwise sequence of the vertex points, and otherwise negative. (Let B_1, B_2, \dots, B_n be a contour point set similar to A_1, A_2, \dots, A_m of Fig. 2.) One can then see that concave contour sections, as for example the point sequence A_3, A_4, A_5, A_6, A_7 , become convex by reversing their sequence. According to the above criterion, the optimal approximation by triangles of this sec-

tion is that which maximizes the volume of the subpolyhedron formed by the reversed point sequence A_7 , A_6 , A_5 , A_4 , A_3 , A_7 or, equivalently, that which minimizes the volume of the polyhedron formed by the sequence A_3 , A_4 , A_5 , A_6 , A_7 , O_A . This last decomposition indicates the general objective function for any contour line subsection—also valid for nonclosed contour lines; the polyhedron, the volume of which is to be maximized (or minimized), is that formed with the origin O_A and O_B of the x-y coordinate system in the contour planes and the contour point subsections of interest. O_A and O_B may be arbitrarily located, since the volumes are algebraically oriented. Figure 2 describes the decomposition of the total polyhedron volume into additive subvolumes and justifies the iterative scheme presented here.

We now show for later use that an elementary expression can be derived for the volume of the polyhedron originated by a fixed triangulation of any contour line. We consider the example shown in Fig. 3. A decomposition of the polyhedron $A_1A_2A_3, \dots, A_mB_1B_2B_3, \dots, B_n$ into pentahedrons $P^a = A_1A_{i+1}B_jO_AO_B$ and $P^b = A_iB_jB_{j+1}O_AO_B$, with i=1 to m and j=1 to n, for the total volume may be written as

$$V_{\text{TOT}} = \sum_{a} \text{Vol } (P^a) + \sum_{b} \text{Vol } (P^b).$$
 (2)

The superscript a represents the pentahedrons having a triangular face $A_iA_{i+1}B_j$ with two vertices from the contour point set S^a , and the superscript b similarly represents the pentahedrons with two vertices B_j and B_{j+1} from the set S^b . A further partitioning of each pentahedron P^a or P^b into tetrahedrons is

$$\begin{split} P^{a}(A_{i}A_{i+1}B_{j}\mathcal{O}_{A}\mathcal{O}_{B}) &= T_{1}^{a}(A_{i}A_{i+1}B_{j}\mathcal{O}_{B}) \\ &+ T_{2}^{a}(A_{i}A_{i+1}\mathcal{O}_{A}\mathcal{O}_{B}), \end{split}$$

$$\begin{split} P^b(A_iB_jB_{j+i}\mathcal{O}_A\mathcal{O}_B) &= T_1^{\ b}(A_iB_jB_{j+1}\mathcal{O}_A) \\ &+ T_2^{\ b}(B_jB_{j+1}\mathcal{O}_A\mathcal{O}_B) \,. \end{split}$$

Equation (2) then becomes a summation over four kinds of tetrahedrons:

$$V_{\text{TOT}} = \sum_{a} \text{Vol} (T_{1}^{a}) + \sum_{b} \text{Vol} (T_{1}^{b}) + c_{a} + c_{b},$$

where the two last terms

$$c_a = \sum_{i=1}^{m-1} \text{Vol} [T_2^a (A_i A_{i+1} O_A O_B)],$$

$$c_b = \sum_{j=1}^{n-1} \text{Vol} [T_2^{\ b}(B_j B_{j+1} O_A O_B)]$$

represent the volume of the two pyramids A_1A_2, \dots, A_mO_B and B_1B_2, \dots, B_nO_A , which are independent of the particular triangulation assumed a priori and are thus constant.

The volume of the tetrahedrons T_1^a and T_1^b is given by

$$\operatorname{Vol} (T_{1}^{a}(A_{i}A_{i+1}B_{j}O_{B})) = \frac{1}{3}(\overrightarrow{O_{B}A_{i}} \times \overrightarrow{O_{B}A_{i+1}}) \overrightarrow{O_{B}B_{j}}$$

$$= v_{ij}^{a}, \qquad (3a)$$

Vol
$$(T_1^b(A_iB_jB_{j+1} O_A)) = \frac{1}{3}(\overrightarrow{O_AB_j} \times \overrightarrow{O_AB_{j+1}}) \overrightarrow{O_AA_i}$$

= v_{ij}^b . (3b)

When the contour points are given by their Cartesian coordinates $A_i = \{X_i^A, Y_i^A, Z^A\}$, i = 1 to m, and $B_j = \{X_j^B, Y_j^B, Z^B\}$, j = 1 to n, we obtain for (3a) and (3b) the formulas

$$v_{ij}^{\ a} = \frac{1}{3}(Z^B - Z^A)(X_i^A Y_{i+1}^A - X_{i+1}^A Y_i^A),$$
 (4a)

$$v_{ij}^{b} = \frac{1}{3} (Z^{B} - Z^{A}) (X_{j}^{B} Y_{j+1}^{B} - X_{j+1}^{B} Y_{j}^{B} + X_{i}^{A} Y_{i}^{B} - X_{i}^{B} Y_{i}^{A}).$$
(4b)

The total volume of the polyhedron, expressed by (2), can be rewritten explicitly, using the formulas (4a) and (4b), as

$$V_{\text{TOT}} = \sum_{i,j} v_{ij}^{\ \ n} + \sum_{i,j} v_{ij}^{\ \ b} + \text{const.}$$
 (5)

Expression (5) is the objective function to maximize for obtaining the optimal triangulation. This formula shows that each triangular face of the polyhedron P contributes additively to the total volume.

Enumeration of all triangulations

We consider the two convex sets of contour points $S^a = \{A_i\}$, i = 1 in m, and $S^b = \{B_j\}$, j = 1 to n, given in Fig. 3. To find an appropriate formulation of the permutational structure of the triangulation, we describe the junctions of points of opposite contour lines to triangles with the help of a binary $n \times m$ matrix $M = \{a_{ij}\}$. M is associated with the sets S^a and S^b such that the matrix element a_{ij} is equal to unity if the ith contour point A_i of the set S^a and the jth contour point B_j of the set S^b are joined, and 0 if they are not. A triangle consists of two junctions A_iB_j and A_iB_k and is represented in this matrix M by two 1-elements. The requirements of the triangulation are described by the following three properties of the matrix elements:

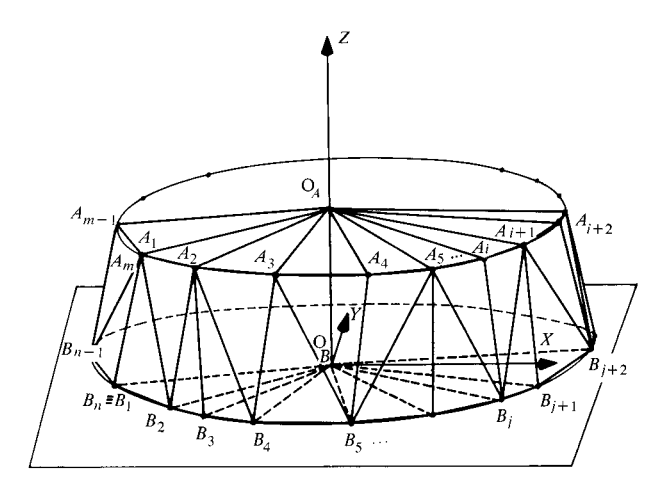


Figure 3 The polyhedron arising through a trial triangulation between two sets of contour points $S^a = \{A_1, A_2, A_3, \dots, A_m\}$ and $S^b = \{B_1, B_2, B_3, \dots, B_n\}$ describing closed convex contour lines.

1. A triangle necessarily shares two consecutive contour points, either in set S^a or in set S^b . This means that

if
$$a_{ij} = 1$$
, then either $a_{i+1, j} = 1$ or $a_{i, j+1} = 1$. (6)

2. Each contour point is joined at least once with a point of the opposite contour. This means that

$$\sum_{i=1}^{m} a_{ij} \ge 1 \text{ and } \sum_{i=1}^{n} a_{ij} \ge 1.$$
 (7)

3. Junctions between the two contour lines cannot cross over. If

$$a_{ij}=1$$
 and $a_{i+1,\ j}=1$, then it must hold that
$$a_{i,\ j+1}=0, \text{ and}$$
 if $a_{ij}=1$ and $a_{i,\ j+1}=1$, then it must hold that
$$a_{i+1},=0. \tag{8}$$

The binary matrix M corresponding to the triangulation of Fig. 3 is explicitly represented to allow for the recognition of these three constraints:

$$M = \begin{cases} i = 1, 2, 3, 4, 5, \cdots m - 2, m - 1, m \\ 1 & 0 & 0 & 0 & 0 & \cdots \\ 1 & 1 & 0 & 0 & 0 & \cdots & 0 \\ 0 & 1 & 0 & 0 & 0 & \cdots & 0 \\ 0 & 1 & 1 & 0 & 0 & \cdots & 0 \\ 0 & 0 & 1 & 1 & 1 & \cdots & 0 \\ & & & & & & & & \\ & & & & & & & \\ & & & & & & & \\ & & & & & & & \\ & & & & & & & \\ & & & & & & & \\ & & & & & & & \\ & & & & & & \\ & & & & & & \\ & & & & & & \\ & & & & & & \\ & & & & & & \\ & & & & & & \\ & & & & & \\ & & & & & \\ & & & & & \\ & & & & & \\ & & & & \\ & & & & \\ & & & & \\ & & & & \\ & & & & \\ & & & & \\ & & & & \\ & & & \\ & & & \\ & & & \\ & & & \\ & & & \\ & & & \\ & & & \\ & & & \\ & & & \\ & & & \\ & & & \\ & & & \\ & & & \\ & & \\ & & \\ & & & \\ & & \\ & & \\ & & & \\$$

5

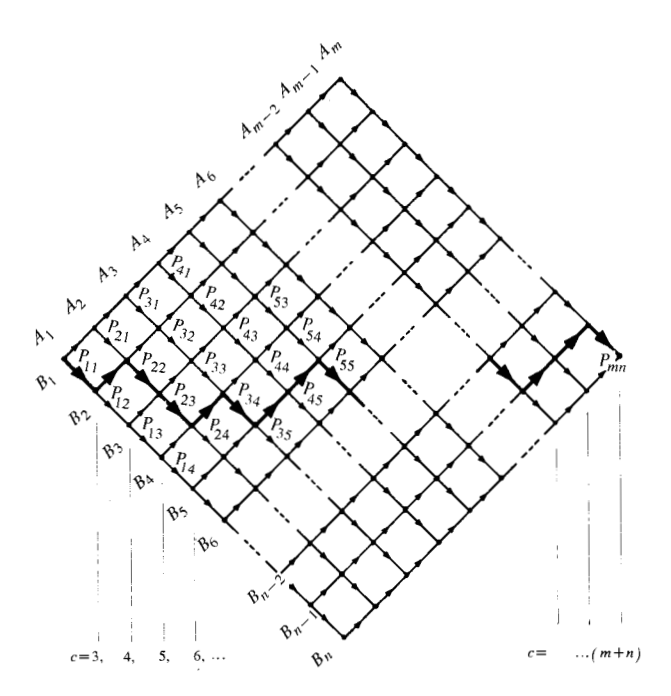


Figure 4 Graph $G = \{P_{ij}, N\}$ associated with the two contour point sets $S^a = \{A_i\}$ and $S^b = \{B_j\}$ of Fig. 3. The triangulation presented in Fig. 3 and the matrix M of formula (9) is indicated in G by the path marked with large arrows from vertex P_{11} to vertex P_{12} .

We see that the partitioning of the side surface of the polyhedron into a fixed triangle arrangement corresponds in the matrix M to a fixed chain of adjacent 1-elements joining a_{11} to a_{mn} and obeying the rules (6) to (8).

The enumeration of all possible triangle permutations is best described by introducing a graph $G = \{P, N\}$ of vertices P and arcs N associated with the matrix M in such a way that each element a_{ij} of the matrix (9) represents a vertex P_{ij} of the graph (see Fig. 4). The double subscript i and j of the vertices should indicate clearly that P_{ij} represents the same item as does the matrix element a_{ij} , namely the segment A_iB_j . It is then evident that an arc $N = (P_{ij}, P_{ik})$ of G, joining any two vertices P_{ij} and P_{ik} , represents the triangle $A_iB_jB_k$. The constraints (6) and (7) restrict the graph G to the arcs $(P_{ij}, P_{i+1, j})$ and $(P_{ij}, P_{i, j+1})$ shown in Fig. 4. Condition (8) is expressed by assigning a direction to the arcs of the graph.

The interpretation of the graph G of Fig. 4 is extremely simple: A sequence of adjacent arcs is called a *path* in graph theory [3]. (Two arcs are said to be adjacent if they have a vertex in common.) Each path joining the vertices P_{11} and P_{mn} represents in G a fixed triangulation. The total number of distinct paths from P_{11} to P_{mn} is the total number of different triangle arrangements. It can be shown that it is given by Eq. (1).

Finding the optimal triangulation

Let us consider further the two convex sets S^a and S^b of contour points in Fig. 3, and the graph G associated with them and shown in Fig. 4. G will be interpreted as a "maximum cost graph" [3] by assigning to each arc $N_{ij} = (P_{ij}, P_{i+1, j})$ or $(P_{ij}, P_{i, j+1})$ a constant value representing the volume v_{ij} of the tetrahedron $A_i A_{i+1} B_j O_B$ or $A_i B_j B_{j+1} O_A$, with i and j running from 1 to m-1 and m-1, respectively. The value of v_{ij} is given either by (4a) or (4b) by

$$v_{ij} = v(N_{ij}) = v(P_{ij}, P_{i+1, j}) = v_{ij}^{\ a}, \text{ or}$$

= $v(P_{ij}, P_{i, j+1}) = v_{ij}^{\ b}.$ (10)

As already shown, the total volume of the polyhedron originated by a triangle arrangement is the objective function to be maximized and can be decomposed additively into the partial tetrahedron volumes associated with each triangular face of the polyhedron. Finding the triangulation which maximizes this polyhedron consists, then, in finding in graph G the path π going from the vertex P_{11} to the vertex P_{mn} such that the expression

$$V(\pi) = \sum_{N_{ij} \in \pi} v(N_{ij}) \tag{11}$$

is maximum. This classical problem of graph theory may be solved in various ways [3]. For the specific simple structure of graph G the following algorithm is easy to realize in a computer.

Each vertex P_{ij} of graph G in Fig. 4 is associated with an index w_{ij} and a pointer p_{ij} . We handle in turn all vertices along a vertical column labeled by a value c = i + j, i.e., a column consisting of the vertices P_{ij} satisfying i + j = c. We progress from left to the right, starting at the vertex column c = 3 and ending at c = m + n.

1. To begin, we set in column c = 3 the indices w_{12} and w_{21} according to (10)

$$\begin{split} w_{12} &= v(P_{1, 1}, P_{1, 2}) = v_{12}^{\ a}, \\ w_{21} &= v(P_{1, 1}, P_{2, 1}) = v_{12}^{\ b}. \end{split}$$

2. For any subsequent column $c = 4, 5, 6, \cdots$ of vertices, we calculate at each vertex P_{ij}

$$V_a = w_{i-1,\ j} + v(P_{i-1,\ j}, P_{ij})$$
, and $V_b = w_{i,\ j-1} + v(P_{i,\ j-1}, P_{ij})$.

The index w_{ij} associated with the vertex P_{ij} is set

$$w_{ij} = \max (V_a, V_b), \tag{12}$$

_

and the pointer p_{ij} connects the current vertex P_{ij} to either vertex $P_{i-1, j}$ or to vertex $P_{i, j-1}$ of the previous column c-1 by setting

$$p_{ij} = \begin{cases} 1 & \text{if } V_a \ge V_b \\ 0 & \text{if } V_a < V_b. \end{cases}$$
 (13)

This pointer p_{ij} acts as an indicator to keep a record in graph G of the path π from vertex P_{11} to vertex P_{ij} giving maximum value for quantity (11). Index w_{ij} contains $V(\pi)$ for this path π .

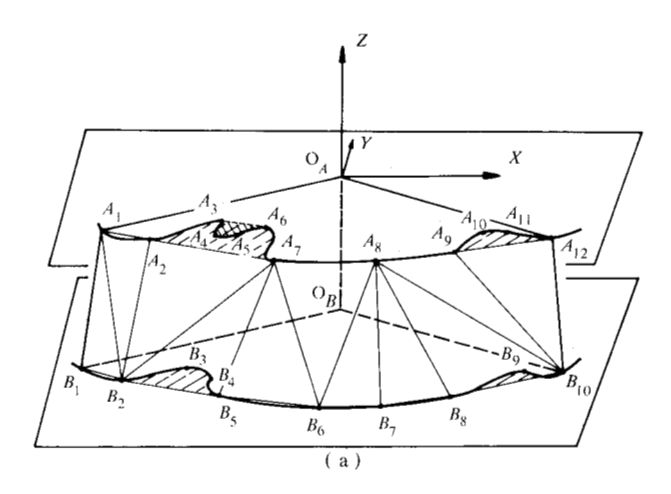
3. The procedure ends as soon as P_{mn} is reached. The path π_{max} from P_{11} to P_{mn} with the maximum $V(\pi_{max})$ value is then backtracked by following the pointers P_{ij} from the vertex P_{mn} to the vertex P_{01} .

The general triangulation algorithm

The computation procedure for optimal triangulation described thus far holds exclusively for pairs of convex contour lines. This procedure, however, is also valid for pairs of concave contour-point subsets, on the premise that the max-operator in Eq. (12) of the algorithm is replaced by a min-operator, since expression (11) is then to be minimized.

The application of this optimization algorithm to contour lines with alternating sign of curvature, as illustrated by Fig. 2, requires a careful adaptation into the iteration scheme previously indicated. The realization of a decomposition procedure that allows the alternating handling of convex and concave contour subsets separately is not obvious. We explain the main lines of the strategy by means of an example. We assume two given sets S_0^a and S_0^b of contour points, but now mixed into convex and concave contour sections. Figure 5(a) will serve us as example for the iterative decomposition of the triangulation process.

- 1. The first step has already been exhaustively treated above: The point subset $S_1^a = \{A_1, A_2, A_7, A_8, A_9, A_{12}\}$ of the upper contour S_0^a and the subset $S_1^b = \{B_1, B_2, B_5, B_6, B_7, B_8, B_{10}\}$ of the lower contour S_0^b provide two convex contour lines for which the algorithm holds literally. The subsets S_1^a and S_1^b are determined by repeated application of the circle test for curvature sign. The graph G associated with the set S_1^a and S_1^b is presented in Fig. 5(b). We assume that the path π_1 traced in G has been obtained by maximizing expression (11). The corresponding triangulation is then entered into Fig. 5(a).
- 2. The second phase of the general algorithm handles the triangulation at the omitted sections of the contour lines. Figure 5(a) illustrates the two principal cases to be distinguished by the selection procedure for the next iteration steps.



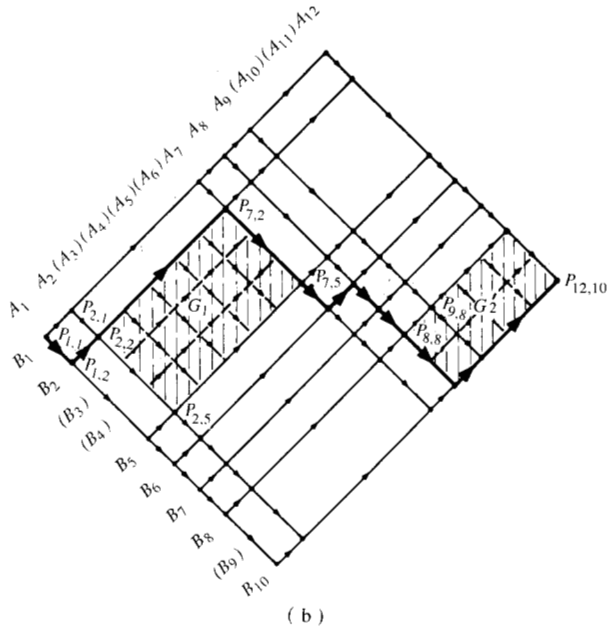


Figure 5 (a), Example of triangulation for the general case of two arbitrarily flexed contour lines defined by $S_0^a = \{A_1, A_2, \cdots, A_{12}\}$ and $S_0^b = \{B_1, B_2, \cdots, B_{10}\}$. (b) Graph associated with the contour-point subsets $S_1 = \{A_1, A_2, A_7, A_8, A_0, A_{12}\}$ and $S_1^b = \{B_1, B_2, B_5, B_6, B_7, B_8, B_{10}\}$ of Fig. 5(a) and taken for the first iteration step of the triangulation algorithm. The path π_1 maximizing the polyhedron volume is indicated by large arrows. The subgraphs G_1 and G_2 handled in the next iteration step are shaded.

In the first case, the points A_2 , A_7 , B_2 , and B_5 which delimit the boundaries of the omitted contour sections are mutually joined by the segments A_2 B_2 and A_7 B_5 . Thus, the point subsets $S_2^a = \{A_2, A_3, A_6, A_7\}$ and $S_2^b = \{B_2, B_3, B_4, B_5\}$ are clearly to be triangulated next. The interpretation by graph G in Fig. 5(b) indicates the computational method. If the vertices $P_{2,2}$ and $P_{7,5}$ are contained in the path π_1 , they delim-

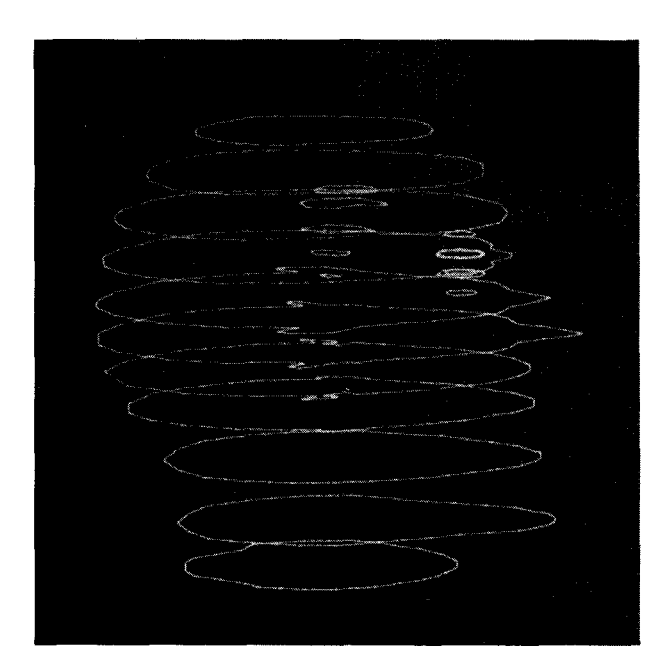


Figure 6 Lateral view on the screen of an IBM 2250 display unit of the contour lines of a head. The contour points in each parallel cross section have been joined to closed polygons.

it a subgraph G1 of G into which a path from the vertex $P_{2,2}$ to the vertex $P_{7,5}$ has to be found next such that the polyhedron $A_2A_3A_6A_7B_2B_3B_4B_5O_AO_B$ has minimum volume. This subgraph, labeled G1, has been shaded in Fig. 5(b).

The second and more confusing case arises when the boundaries A_9 and A_{12} of the omitted upper contour section are not connected with the respective limits B_8 and B_{10} of the lower contour. The junctions A_8B_{10} (instead of A_9B_8) and $A_{12}B_{10}$ delimit here the contour portion to be handled in the second iteration step. The further concave subsets are $S_2^{\ a'} = \{A_8, A_{10}, A_{11}, A_{12}\}$ and $S_2^{\ b'} = \{B_8, B_9, B_{10}\}$. The second subgraph, G_2 , to be handled is delimited by the vertices $P_{8, 8}$ —not $P_{9, 8}$ as in the previous case—and $P_{12, 10}$. G_2 has also been shaded in Fig. 5(b). The recognition by the computer program of the vertex $P_{8, 8}$ instead of $P_{9, 8}$ as a limit of the subgraph G_2 requires careful programming, the details of which we do not present here.

3. The last iteration step finally resolves the triangulation of the remaining convex contour portion $S_3^a = \{A_3, A_4, A_5, A_6\}$. Since no corresponding convex contour section exists in S_0^b , the triangulation assignment becomes obvious in this case.

Triangulation of the contours of a human head

The triangulation method presented in this paper has been implemented, in conjunction with the radiological clinic at the University of Heidelberg, in a research experimental computer program for three-dimensional planning of radiation therapy [4]. The major feature of this approach consists in creating a triangulated model of all relevant anatomical surfaces involved in the treatment. The triangulation is done by a FORTRAN subroutine that accepts patient contour measurements in form of a set of Cartesian x-y coordinates at cross sections of constant z value.

To illustrate the practical details of calculation by example, we describe the main phases of the triangulation of a human head. Figure 6 shows, projected on the screen of an IBM 2250 display unit, the initial contour points input to the computer. To enhance the presentation, consecutive points have been joined by closed contour lines, and the coordinate system into which the contour points were measured has been rotated laterally in order to present the contour lines in a convenient overview.

To realize the triangulated model, the program handles in turn each pair of adjacent contour lines. We then restrict our discussion of the algorithm to only one pair of contour lines. We concentrate our attention on the triangulation of the fifth and sixth cross sections from the bottom of Fig. 6. These two contour lines are shown in Fig. 7. The choice of this pair has been made to illustrate the way a correct triangulation is realized in a complicated region such as that of the ears.

The program starts the triangulation procedure by initializing a binary matrix for Eq. (9) with the entries in the rows and the columns denoting the contour points of the upper and the lower cross section, respectively. This matrix is permanently reserved in storage until the triangulation of the contour pair is achieved.

Accordingly, in the iteration procedure of the algorithm, the program has to select for the first iteration step that subset of contour points which yields a purely concave contour polygon for both sides. The repeated application of the circle test to convex contour sections permits only the points shown in Fig. 8 to be retained. The triangulation of the removed points is resumed during later iteration steps.

To describe, according to the equations (6) to (9), all possible triangle junctions between contour points of the two contour lines, a binary matrix is associated with them. This 14×18 matrix is shown in Fig. 9. Columns and rows are labeled according the subscripts of the points of Fig. 8. The matrix shows the result of the minimum-path algorithm that maximizes the volume of the polyhedron delimited by the pair of cross sections. The binary values of the matrix elements are conventionally

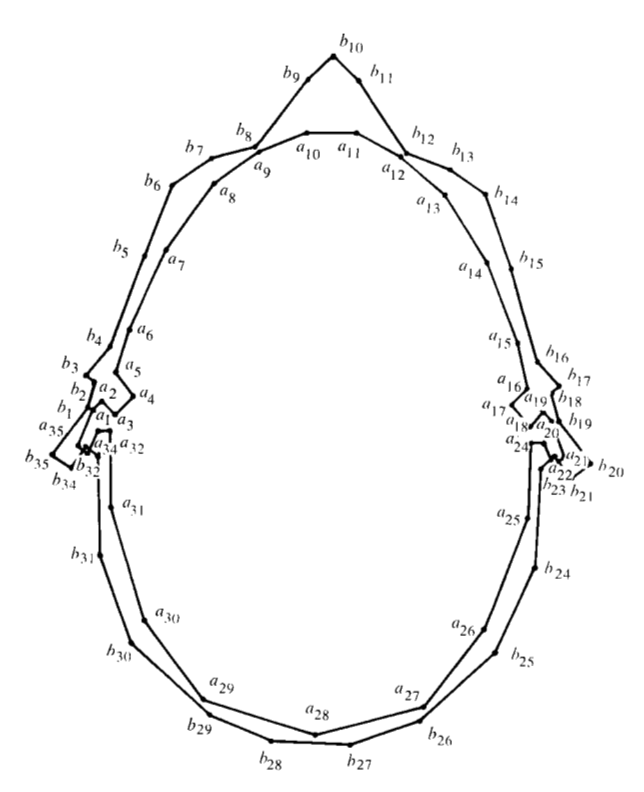
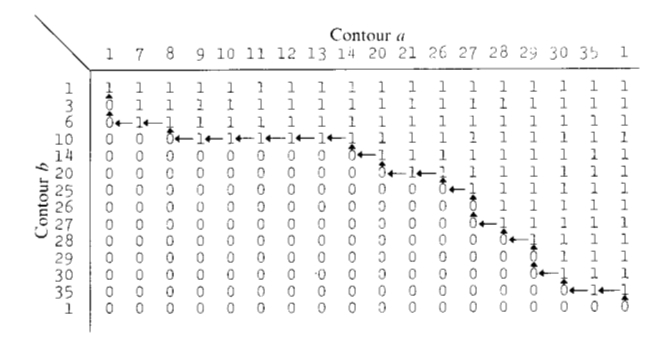


Figure 7 Two adjacent contour lines from the head in Fig. 6.

fixed such that $p_{ij}=1$ means a pointer "backwards" in the matrix, i.e., it specifies the triangle a_i $a_{i-1}b_j$; the value $p_{ij}=0$ on the other hand, indicates a pointer "upwards", i.e., it specifies the triangle a_i b_j b_{j-1} . Tracking back in the matrix from the lower-right to the upper-left element yields the optimal triangle partitioning of Fig. 8.

The only significant permanent storage requirement for the algorithm is the binary matrix of Fig. 9. In practice that matrix is realized in computer memory as the initially defined large matrix shown in Fig. 10: Col-

Figure 9 The binary matrix of Eq. (9) describing for Fig. 8 the junctions of contour points to triangles. The matrix element values result from the shortest path algorithm. The value $p_{ij} = 1$ specifies the triangle $a_i a_{i-1} b_j$, the value $p_{ij} = 0$ specifies the triangle $a_i b_j b_{j-1}$. The chain of pointers which tracks back in the matrix from the lower right element to the upper left indicates the optimal triangulation.



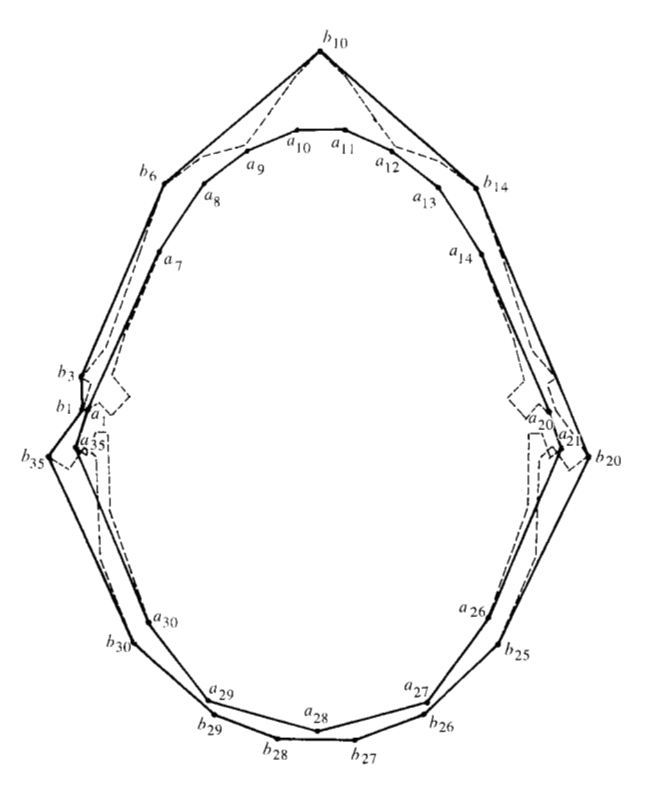
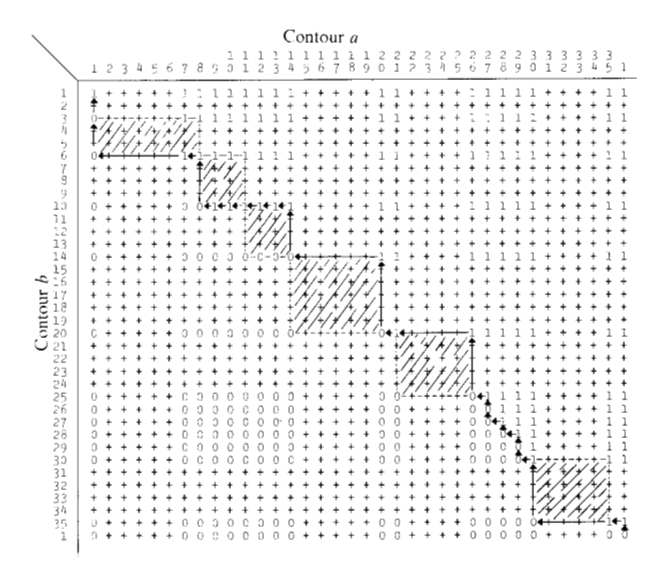


Figure 8 Contour points selected from Fig. 7 for the first iteration of the triangulation. The points a_1 and b_1 are assumed to correspond a priori.

Figure 10 The binary matrix of Eq. (9) set up in computer memory to perform the triangulation of Fig. 7. The figure shows the state of the matrix at the end of the first iteration step. Rows and columns of deferred contour points are filled up with the character '+'. The 1 and 0 values correspond to the matrix of Fig. 9. The pointer chains specify the optimal triangulation and delimit six shaded submatrices which are to be processed in the next iteration.



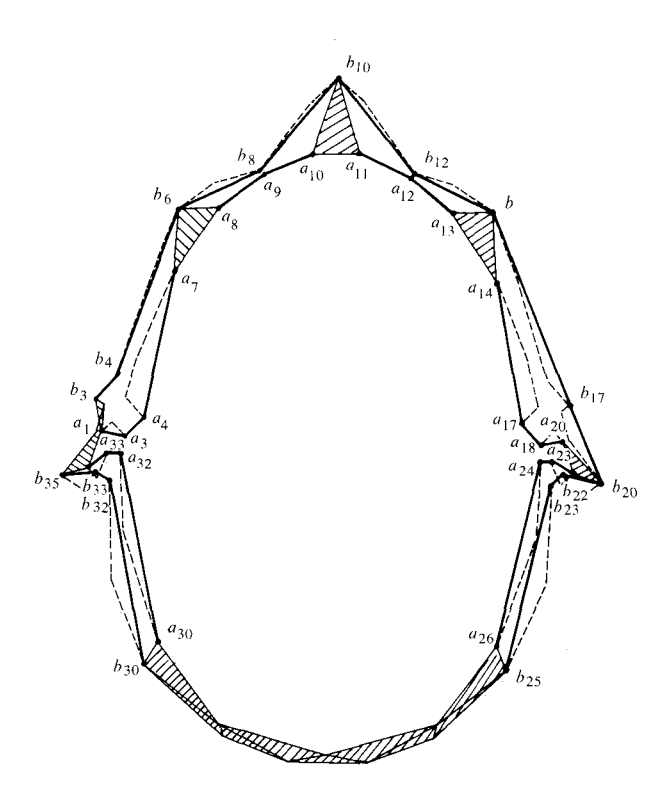


Figure 11 Convex contour sections handled during the second iteration of the triangulation. Each section corresponds to a shaded submatrix in Fig. 10. Definitively fixed triangles resulting from the previous iteration are indicated in the drawing.

umns and rows corresponding to deferred contour points are crossed out to show the state of the matrix during the first iteration step. The backtrack chain of pointers in Fig. 10 permits determination of the remaining contour sections that are candidates for the next iteration steps. The program determines all occurrences of pointer "jumps" over deferred rows and columns. Two consecutive jumps delimit a submatrix that corresponds to a nontriangulated contour section pair. In Fig. 10, six submatrices have been recognized by the program. They correspond to six separate convex contour sections to be handled next; these are shown in Fig. 11. The program processes this second iteration step in nearly complete analogy to the first one and can loop over the same program section.

The triangulation is completed at the end of the third iteration step. This last step handles only the remaining short concave sections visible on Fig. 11. The backtrack chain of binary pointers is then complete in the matrix of Fig. 10. The program finally generates the corresponding list of contour point triples, which indicates the final triangulation obtained for the considered pair of cross sections.

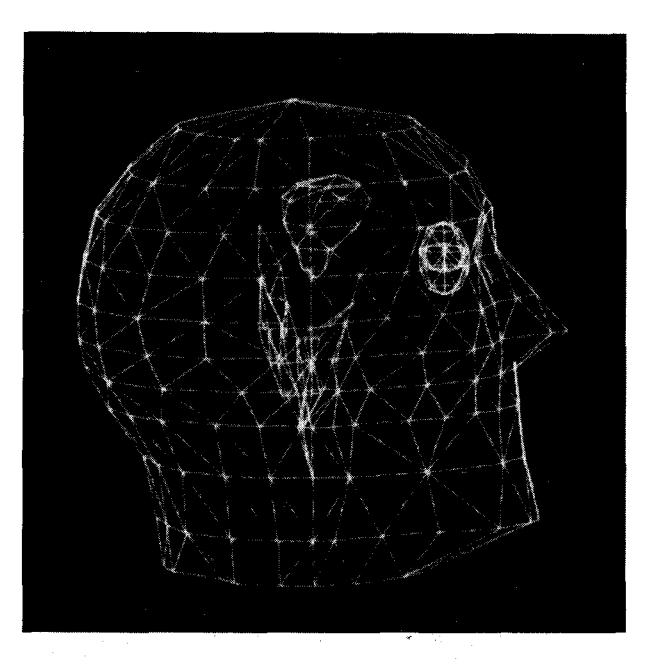


Figure 12 Result of the triangulation of Fig. 6 as displayed on the video terminal.

Figure 12 shows the three-dimensional representation of the totally triangulated contour lines of Fig. 6. One may note the removing of the hidden triangles from the display screen. The most useful property of the triangulated model is to provide a description of surfaces particularly well adapted for graphical visualization on a display terminal. The possibility of manipulating three-dimensional anatomical figures under visual control motivated the development of the planning system in a highly interactive way. The accuracy of any particular representation depends on how many contour lines are used to describe the three-dimensional object, how many contour points are selected for each line, and how they are distributed.

Acknowledgment

The author is indebted to W. A. Hunt for having directed his attention to the subject of this paper.

References and note

- 1. Computers in Radiology, Proceedings of the Fourth International Conference on the Use of Computers in Radiation Therapy, Uppsala, Sweden, August 7-11, 1972.
- 2. To the best of our knowledge no publication exists on this subject. In the field of biomedicine, the triangulation technique was proposed by several researchers, of which Dr. U. Rosenow (Göttingen, W. Germany) and Dr. J. Weinkam (St. Louis, USA) are known to the author. Dr. W. A. Hunt (IBM Houston, USA) elaborated upon a triangulation method which fails, however, for complex surfaces.

- 3. C. Berge, The Theory of Graphs and Its Applications, John
- Wiley and Sons, Inc., New York, 1967.
 M. Bergen and E. Keppel, "A Comprehensive System for Interactive Planning in Radiation Therapy," *Technical Report* 72.01.001, IBM Scientific Center, Heidelberg, Germany, 1972.

Received June 5, 1973; Revised June 5, 1974

The author is located at the IBM Heidelberg Scientific Center, Tiergartenstrasse 15, 6900 Heidelberg, Germany.